

# CDistNet: Perceiving Multi-Domain Character Distance for Robust Text Recognition

Tianlun Zheng · Zhineng Chen\* · Shancheng Fang · Hongtao Xie · Yu-Gang Jiang

Received: date / Accepted: date

**Abstract** The Transformer-based encoder-decoder framework is becoming popular in scene text recognition, largely because it naturally integrates recognition clues from both visual and semantic domains. However, recent studies show that the two kinds of clues are not always well registered and therefore, feature and character might be misaligned in difficult text (e.g., with rare shapes). As a result, constraints such as character position are introduced to alleviate this problem. Despite certain success, a content-free positional embedding hardly associates stably with meaningful local image regions. In this paper, we propose a novel module called Multi-Domain Character Distance Perception (MDCDP) to establish a visual and semantic related positional encoding. MDCDP uses positional embedding to query both visual and semantic features following the attention mechanism. The two kinds of constrained features are then fused to produce a reinforced feature, generating a content-aware embedding that well perceives spacing variations and semantic affinities among characters, i.e., multi-domain character distance. We develop a novel network named CDistNet that stacks multiple MDCDPs to guide a gradually precise distance modeling. Thus, the feature-character alignment is well built even various recognition difficulties presented. We create two series of augmented datasets with increasing recognition difficulties and apply CDist-

tNet to both them and six public benchmarks. The experiments demonstrate that CDistNet outperforms recent popular methods by large margins in challenging recognition scenarios. It also achieves state-of-the-art accuracy on standard benchmarks. In addition, the visualization shows that CDistNet achieves proper information utilization in both visual and semantic domains. Our code is given in <https://github.com/simplify23/CDistNet>.

**Keywords** Scene Text Recognition, Attention Mechanism, Positional Embedding, Character Distance

## 1 Introduction

Scene text recognition aims to read text in natural images. It has attracted wide interest due to its pivotal role in extracting high-level textual information that is critical for many vision-related applications. Although extensive studies are carried out with significant progress over the past years (Baek et al., 2019; Fang et al., 2021; Lee and Osindero, 2016; Shi et al., 2017), the task still remains challenging for several difficulties, e.g., complex text deformations, unequally distributed characters, multiple fonts, cluttered background, etc. How to tackle these challenges is becoming a key issue for modern text recognizers.

Recently, Transformer-based encoder-decoder methods attain impressive performance in this task. For example, Sheng et al. (Sheng et al., 2019) extract visual feature from the text image, and inject semantic feature from the annotations to the decoder side. During decoding, the text image is identified character-by-character. At each time step, the semantic feature first concatenates with a sinusoidal positional embedding, and then is used as the *query* vector to align its correspondence

T. Zheng, Z. Chen and Y.G. Jiang are with School of Computer Science and Shanghai Collaborative Innovation Center of Intelligent Visual Computing, Fudan University, Shanghai 200438, China. (E-mail: tlzheng21@m.fudan.edu.cn, zhinchen@fudan.edu.cn, ygj@fudan.edu.cn)

S. Fang and H. Xie are with School of Information Science and Technology, University of Science and Technology of China, Hefei 230026, China. (E-mail: fangsc@ustc.edu.cn, htjie@ustc.edu.cn)

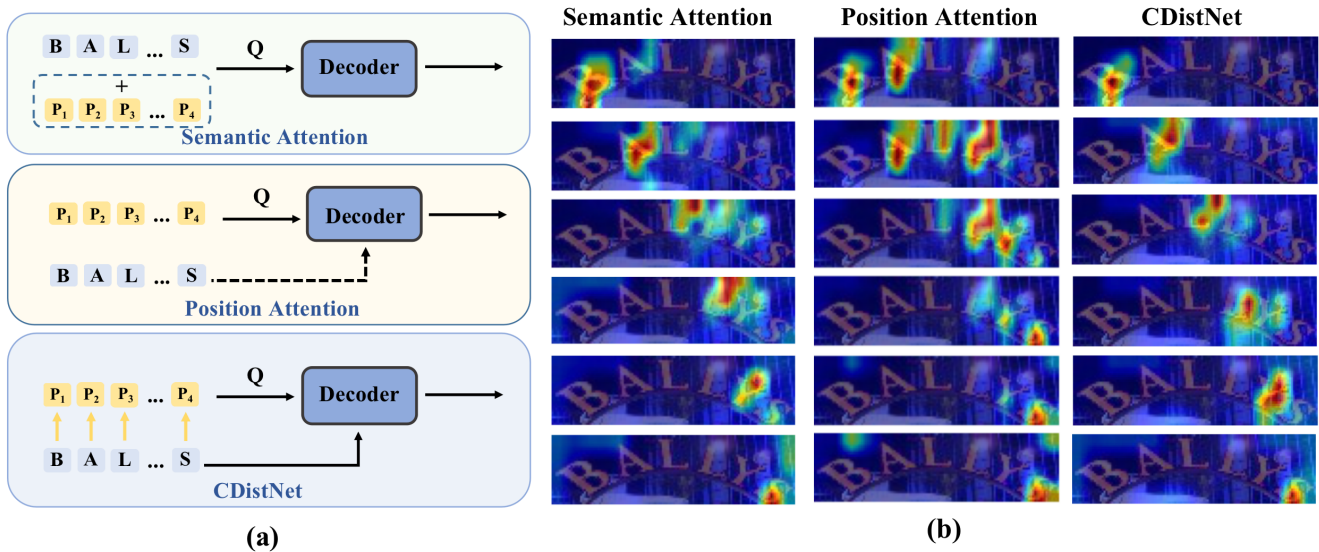


Fig. 1: **Semantic Attention** (Li et al., 2019; Sheng et al., 2019; Shi et al., 2018; Wang et al., 2019a): the semantic feature is employed as the query for attention modeling. It easily causes *attention drift*. (the first column in (b), line 3,4); **Position Attention** (Fang et al., 2021; Wang et al., 2021; Yu et al., 2020; Yue et al., 2020): using a fixed positional embedding as the query, it may wrongly attend multiple characters in one time step. (the second column in (b), line 1,2,3); **CDistNet**: the positional embedding also interacts with semantic feature, resulting in proper attention localization (the third column in (b)). Dotted line and box are optional. The visual branch is omitted in (a) for simplicity.

in the visual space, by which a character-level recognition decision is derived. The pipeline can be summarized as the semantic attention scheme (Baek et al., 2019; Qiao et al., 2020; Sheng et al., 2019), as shown in the top part of Fig.1(a). It has advantages such as providing a unified way of integrating recognition clues from both visual and semantic domains, which is then used to align the character to be recognized in the text image. However, recent studies (Wang et al., 2020; Yue et al., 2020) show the two kinds of clues depend on each other. It is explained as when one of the two clues is weak, the other could not stably find its counterpart. Therefore, feature and character are easily mismatched in difficult text such as with rare shapes or perspective text. Moreover, it is also observed in (Yue et al., 2020) that the mismatch is more prevalent in long text. Since the semantic feature is gradually reinforced and dominates the recognition with the accumulation of decoded characters, features between neighbor time steps become similar, easily causing *attention drift* (see the first column of Fig.1(b), line 3,4) (Cheng et al., 2017; Liao et al., 2019; Wan et al., 2020; Wang et al., 2019b) and degraded accuracy.

In view of the problem above, several studies (Fang et al., 2021; Wan et al., 2020; Yu et al., 2020; Yue et al., 2020) decouple position and semantic features by employing a single positional branch for additional atten-

tion catching (see the middle part of Fig.1(a)). It generates the so-called position attention scheme. These methods alleviate the mismatch somewhat and get improved accuracy. Nevertheless, their positional embedding is *content-free*, where a fixed embedding is employed to associate with visual features of different text images. It is more like a placeholder constraint rather than content-aware receptor, which can't represent the diverse character patterns appearing in a fixed position and generates sub-optimal representation. We observe that it may wrongly attend multiple characters in one time step, as shown in Fig.1(b) (the second column, line 1,2,3). Although the later fusion of it with the semantic branch can suppress the drawback to some extent (Yue et al., 2020), the position utility is underestimated by this placeholder-like usage.

More specifically, we argue that more robust feature-character alignments could be reached by modeling feature interactions among visual, semantic and position spaces, which is barely considered in existing studies. Besides being aware of the character spatial position, the position can also be utilized to delineate the character semantic affinity. Moreover, combining the clues is likely to generate a *content-aware* embedding that is aware of both spacing variations and semantic affinities among characters. It is vividly understood as describing the character distance in both visual and semantic

domains, i.e., multi-domain character distance. Therefore, such a joint representation is in favor of perceiving accurate character positions especially in challenging recognition scenarios.

In this paper, we develop a novel module called *Multi-Domain Character Distance Perception* (MDCDP) to overcome the aforementioned issues. Similar to existing studies (Vaswani et al., 2017; Yue et al., 2020), MD-CDP is initialized with a fixed positional embedding. But differently, the embedding is used to *query* both visual and semantic features following the cross-attention mechanism. Therefore, it does not only impose position enhancement on the visual domain, but also describes the character dependence in the semantic domain. By further merging features from both domains, it generates a new *content-aware* embedding that well perceives spatial and semantic distance among characters (see the bottom part of Fig.1(a)). The embedding is then used as the *query* vector of the next MDCDP, to obtain a more attention-focused feature-character alignment. Following this idea, we propose a novel architecture named CDistNet that stacks MDCDP several times to guide a gradually precise character distance modeling. As seen in the third column of Fig.1(b), CDistNet accurately localizes the characters. It ensures that, at each time step, the correct feature is utilized for character decoding, therefore benefiting the recognition especially complex character spatial variations presented.

To evaluate CDistNet, we first create two series of datasets by augmenting the ICDAR2013 benchmark (Karatzas et al., 2013) with horizontal and curved stretching of varying intensities. The generated datasets are termed HA-IC13 (horizontal) and CA-IC13 (curved) series, which have increasing recognition difficulties as the deformation intensity increases. Based on this, extensive experiments are conducted on both the augmented datasets and public benchmarks. In the former, CDistNet attains greater advantages as the deformation intensity rises when compared to recent popular methods, showing its superiority in handling difficult text. While on six popular regular and irregular text benchmarks, CDistNet achieves state-of-the-art recognition accuracy among the competitors. The results demonstrate the effectiveness of establishing a feature representation that is aware of the multi-domain character distance. We also visualize the visual attention map and the semantic affinity matrix during decoding. Generally, they show that not only a proper visual attention localization is obtained, but also a more complete character-involved semantic inference is observed. Both explain the accuracy gain.

Contribution of this paper is threefold. First, we propose MDCDP that employs position feature to *query*

both visual and semantic features, the first attempt that establishes the cross-attention between position and semantic spaces. It enables a *content-aware* embedding that jointly takes into account visual, semantic and position feature. Second, we develop CDistNet, a novel scene text recognizer. It stacks multiple MD-CDPs to well perceive the multi-domain character distance and thus builds robust feature-character alignments, benefiting the recognition especially for difficult text. Third, we carry out extensive experiments and compare CDistNet with existing leading methods. It not only achieves state-of-the-art recognition accuracy, but also shows obvious advantages in challenging recognition scenarios. In addition, the visualization implies that CDistNet achieves proper information utilization in both visual and semantic domains.

## 2 Related Work

Scene text recognition is a long-standing computer vision task intensively studied over decades. Comprehensive surveys can be found in (Chen et al., 2021; Long et al., 2021; Ye and Doermann, 2014). Recently, research efforts mainly lie in irregular text while sequence-based methods become popular (Baek et al., 2019; Bhunia et al., 2021; Cheng et al., 2018; Jaderberg et al., 2016; Luo et al., 2021; Lyu et al., 2018; Nguyen et al., 2021; Rodriguez-Serrano et al., 2015), as different recognition clues (e.g., visual, semantic) can be jointly modeled to get the prediction. Based on how these clues are utilized, we can broadly categorize them into semantic-free, semantic-attention, and position-attention methods.

### 2.1 Semantic-free Methods

Sequence-based methods advance traditional character segmentation-based methods (Bai et al., 2014; Jaderberg et al., 2016) in avoiding the difficult character segmentation problem, while allowing relationships between local image regions as well as semantic information to be mined. Earlier methods in this branch are semantic-free methods. They implement the recognition by utilizing image visual features mainly, while the semantic relationship among characters is not explicitly modeled. For example, Shi et al. (Shi et al., 2017) proposed the CTC-based method, where the visual feature extracted by CNN was reshaped as a feature sequence and then modeled by RNN and CTC loss. Following this pipeline, several methods were developed with improved accuracy by developing a deep-text recurrent network (He et al., 2016), ensembling multiple

RNNs (Su and Lu, 2017), devising a graph convolutional network guided CTC decoding (Hu et al., 2020), etc. Rather than decoding by RNN, segmentation-based methods (Li et al., 2017; Liao et al., 2019; Xing et al., 2019) regarded the recognition as a standard or modified segmentation problem where each character is a target category. However, they generally required character level annotations which were not always readily available. While they are also sensitive to segmentation noisy. In sum, the performance of semantic-free methods was limited, partly due to not directly modeling other recognition clues.

## 2.2 Semantic-attention Methods

Semantic-attention methods (Chen et al., 2020; Luo et al., 2019; Sheng et al., 2019; Shi et al., 2018) utilize the semantic clue to reinforce the visual feature and generally using the attention-based encoder-decoder framework. Lee et al. (Lee and Osindero, 2016) first introduced the attention mechanism into scene text recognition. It employed both the 1D image feature sequence and the embedding of character sequence, by which the semantic clue was leveraged. Later, it was extended by designing a more natural 2D image feature (Li et al., 2019), adding dedicated attention enhancement modules (Cheng et al., 2017), etc. By substituting RNN with Transformer (Vaswani et al., 2017), a powerful model in capturing global dependence in vector sequence, many variants (Lyu et al., 2019; Sheng et al., 2019; Wang et al., 2019a) were developed with improved accuracy. Note that the position encoding was commonly applied to Transformer-based models whose attention mechanism was non-local. For example, sinusoidal positional embedding was employed to record the character position in (Sheng et al., 2019). The embedding is then appended to the semantic feature vector as an auxiliary clue. Later, learnable embedding was developed to adaptively utilize the positional clue in (Devlin et al., 2019; Lan et al., 2019). Despite great processes made, it was observed that there was misalignment between feature and character (i.e., local image region) especially in long text, i.e., *attention drift* (Cheng et al., 2017; Liao et al., 2019; Wang et al., 2019b; Yue et al., 2020).

## 2.3 Position-attention Methods

Position-attention methods emphasize developing a dedicated character position branch to ease the recognition, which has been taken into account by several recent methods. To suppress *attention drift*, TextScanner (Wan et al., 2020) proposed a position order seg-

mentation map to ensure that characters were read in the right order and separated properly. RobustScanner (Yue et al., 2020) proposed a dedicated position enhancement branch along with a dynamic fusion mechanism, then the characters were decoded sequentially and achieved impressive results. Meanwhile, several parallel decoding efforts were conducted by introducing semantic loss of different forms (Fang et al., 2021; Qiao et al., 2020; Wang et al., 2021), where a placeholder sequence was initialized and learned to describe the corresponding characters. Our work falls into the category of position-attention-based sequential decoding. However, different with (Yue et al., 2020) that the positional embedding is *content-free* while only queries the visual feature, we inject the positional embedding to both visual and semantic features, thus characterizing character distance in both domains. They are then further fused to establish an attention-focused feature-character alignment. Moreover, an iterative reinforcement structure is developed for a more precise distance modeling. Our work thoroughly integrates the recognition clues among visual, semantic and position spaces. Therefore, it makes the recognition easier, especially for difficult text.

## 3 Methodology

The proposed CDistNet is illustrated in Fig. 2. It is an end-to-end trainable network that falls into the Transformer-based encoder-decoder framework. Specifically, the encoder consists of three branches, respectively for encoding visual, position and semantic information. On the decoder side, the three kinds of information are fused by a dedicated designed MDCDP module, in which the positional branch is first leveraged to query both visual and semantic features. Then they are fused to generate a reinforced embedding, which records the distance between characters in both visual and semantic domains. It is used as the positional embedding of the next MDCDP to guide a more accurate distance modeling. The MDCDP is stacked several times in CDistNet to achieve a precise feature-character alignment. At last, characters are decoded sequentially based on the output of the last MDCDP.

### 3.1 Encoder

**Visual Branch.** The visual branch utilizes Thin-plate-splines (TPS) as a preprocess to rectify the text image (Baek et al., 2019; Shi et al., 2018). Then, similar to (Fang et al., 2021; Yu et al., 2020), ResNet-50 and Transformer unit are employed as the backbone, which

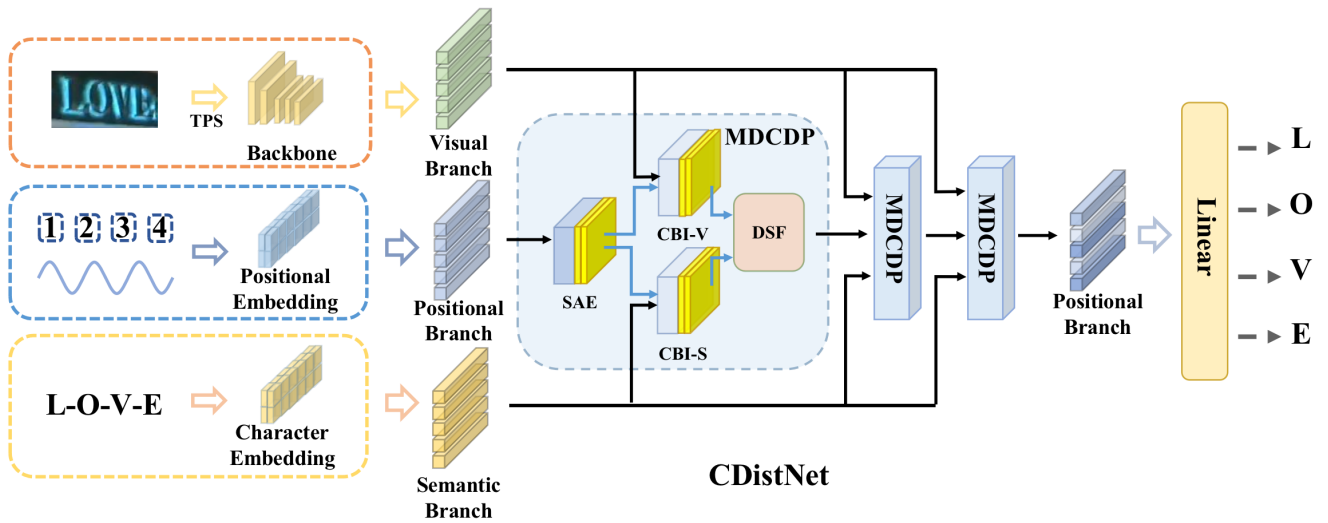


Fig. 2: An overview of the proposed CDistNet. The encoder consists of visual, semantic and positional branches. The three kinds of features are fed into the *Multi-Domain Character Distance Perception* (MDCDP) module that learns a content-aware representation. SAE, CBI and DSF are proposed blocks. CDistNet stacks three MDCDPs to get a gradually precise distance modeling. Output of the last MDCDP is leveraged to decode the characters sequentially.

captures both local and global feature dependencies. The same ResNet-50 as in (Shi et al., 2018; Wang et al., 2020) is used. Besides, the Transformer unit is a three-layer self-attention encoder with 1024 hidden units per layer. The process can be described using the following formula.

$$\mathbf{F}_{\text{vis}} = \tau(\mathcal{R}(\mathbb{T}(I))) \in \mathbb{R}^{N \times P \times E} \quad (1)$$

where  $I \in \mathbb{R}^{W \times H}$  denotes the input text image,  $\mathbb{T}$  is the TPS block.  $\mathcal{R}$  denotes ResNet-50 and  $\tau$  is the Transformer unit.  $N$  and  $E$  are batchsize and the channels of visual feature.  $P = \frac{WH}{64}$  is the length of reshaped visual feature. Both the width and height are shrank to 1/8 of the original size.

**Semantic Branch.** Similar to (Sheng et al., 2019; Yue et al., 2020), the semantic branch encodes the character labels during training or already decoded characters during inference. In training, the character labels are represented as a sequence of word embedding  $\mathbf{F}_{\text{sem}} \in \mathbb{R}^{N \times T \times E}$ , where  $T$  is the number of characters and the feature is decoded in parallel for training acceleration. While in inference, since the character number is unknown in advance, a start token  $\mathbf{F}_{\text{sem}}^0 \in \mathbb{R}^{N \times 1 \times E}$  is defined as the semantic embedding at time step 0. It is used to decode the first character and generates  $\mathbf{F}_{\text{sem}}^1 \in \mathbb{R}^{N \times 2 \times E}$ , where embedding of the just decoded character is appended. Then  $\mathbf{F}_{\text{sem}}^1$  is applied to decode the next character. Following this scheme,  $\mathbf{F}_{\text{sem}}^t \in \mathbb{R}^{N \times (t+1) \times E}$  is obtained when decoding the  $t$ -th character. The whole process is terminated when the

end token is decoded. Therefore, the semantic feature is updated at every time step.

**Positional Branch.** Similar to the semantic branch, the positional branch encodes feature in one-time during training while the feature is updated step-by-step during inference. To encode the character positions in training, we first generate a sequence of vectors each with a fixed constant in its position-indexed dimension while 0 otherwise. Then, the same sinusoidal positional embedding as in (Vaswani et al., 2017) is applied, followed by two MLP layers to get the embedding  $\mathbf{F}_{\text{pos}} \in \mathbb{R}^{N \times T \times E}$ . While in inference, the positional embedding is initialized with a placeholder  $\mathbf{F}_{\text{sem}}^1 \in \mathbb{R}^{N \times 1 \times E}$  as described in training. It then grows with the accumulation of decoded characters, where  $\mathbf{F}_{\text{pos}}^t \in \mathbb{R}^{N \times t \times E}$  defines the embedding of the  $t$ -th time steps. Note that the positional embedding has no start or end token.

### 3.2 MDCDP

We then explain how the MDCDP module is formulated on the decoder side. MDCDP consists of three parts, a self-attention enhancement (SAE) for position feature reinforcement, a cross-branch interaction (CBI) that utilizes position feature to *query* both the visual and semantic branches, obtaining position-enhanced representations, and a dynamic shared fusion (DSF) to get a visual, semantic and positional joint embedding. As a result, the three features are fused and a *content-aware* representation is obtained. An illustrative figure of MD-

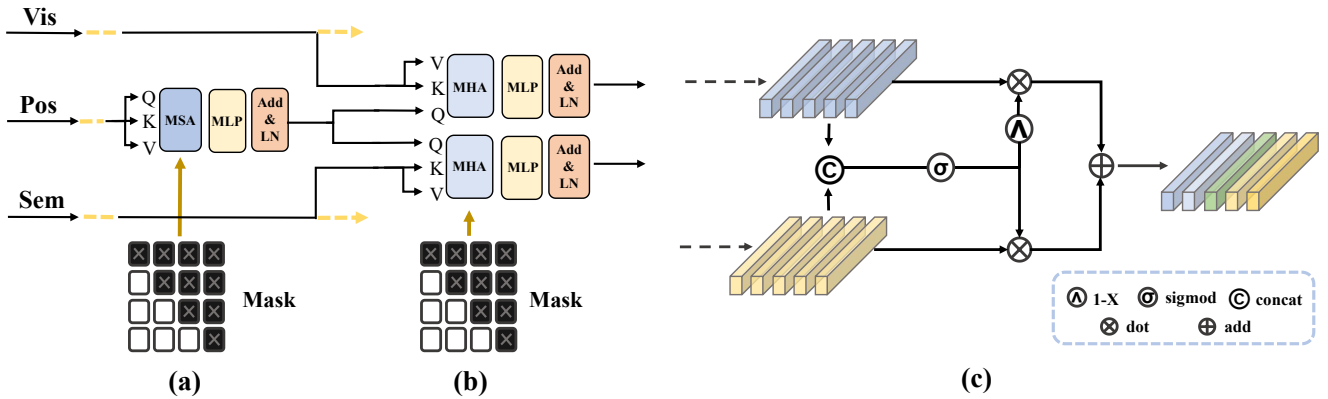


Fig. 3: Details of the MDCDP module. (a) Self-Attention Enhancement (SAE), (b) Cross-Branch Interaction (CBI) and (c) Dynamic Shared Fusion (DSF).

CDP is shown in Fig.3, where details of SAE, CBI and DSF blocks are depicted. From the figure we can get an intuitive understanding of the MDCDP, e.g., how *Query* (Q), *Key* (K) and *Value* (V) are applied.

**Self-Attention Enhancement (SAE).** At time step  $t$ , with the positional embedding  $\mathbf{F}_{pos}^t$  from the encoder, SAE is applied at first to reinforce the embedding using one multi-head attention block (Vaswani et al., 2017) but half its dimension to reduce the computational cost. In addition, an upper triangular mask  $\mathbf{M}_{pos}^t$  is applied to the query vector to prevent from "seeing itself", or saying, leaking information across time steps, which happens in the second and subsequent MDCDPs. This operation is formulated as:

$$\mathbf{F}_{pos}^t = \text{Atten}([\mathbf{F}_{pos}^t, \mathbf{F}_{pos}^t], \mathbf{M}_{pos}^t) + \text{FFN} \quad (2)$$

where FFN represents the feed forward network. Atten is the multi-head attention. The first term in the square bracket is Q, while the second term represents both K and V. In this case is multi-head self-attention.

Note that previous studies (Fang et al., 2021; Yu et al., 2020) did the enhancement on visual branch rather than positional branch. We argue that visual feature from the encoder side is powerful enough. Alternatively, SAE enables a more targeted positional embedding through gradient back-propagation. It leads to a more reasonable feature utilization especially for the second and subsequent MDCDPs.

**Cross-Branch Interaction (CBI).** The enhanced positional embedding  $\mathbf{F}_{pos}^t$  is then treated as the query vector and fed into the visual and semantic branches in parallel. When applied to the semantic branch, we call it CBI-S, and  $\mathbf{F}_{pos\_sem}^t$ , the cross-attention between position and semantic feature is calculated. It simulates the semantic affinity between previously decoded characters and the character to be recognized. Similarly,  $\mathbf{M}_{pos}^t$  is leveraged to prevent the semantic infor-

mation leaking across time steps. Meanwhile,  $\mathbf{F}_{pos\_vis}^t$ , the cross-attention between position and visual feature, is also generated on the CBI-V side. It is explained as using the previously decoded character positions to search for the character region to be recognized in the text image. Thus, both branches are strengthened after the interactions. The two cross-attention operations are defined as:

$$\mathbf{F}_{pos\_sem}^t = \text{Atten}([\mathbf{F}_{pos}^t, \mathbf{F}_{sem}^t], \mathbf{M}_{pos}^t) + \text{FFN} \quad (3)$$

$$\mathbf{F}_{pos\_vis}^t = \text{Atten}([\mathbf{F}_{pos}^t, \mathbf{F}_{vis}^t]) + \text{FFN} \quad (4)$$

Note that previous studies (Baek et al., 2019; Li et al., 2019) used semantic feature as the query to interact with visual feature, a means of establishing the visual-semantic correspondence that is in favor of finding the character to be recognized. RobustScanner (Yue et al., 2020) extended it by adding an additional query from position feature to visual feature and enables a position-enhanced decoding. However, the query is *content-free* and does not interact with the semantic branch. In contrast, we formulate the interactions as the position-based enhancement to both visual and semantic domains. It reinforces not only visual but also semantic features and can be understood as delineating both spatial variations and semantic affinities among characters.

**Dynamic Shared Fusion (DSF).** DSF aims to fusing the two position-enhanced features efficiently and effectively. It takes the two features as input. They are concatenated to form a hybrid feature whose channels are doubled. Then, the feature undergoes a  $1 \times 1$  convolution that encourages feature fusion while halves the channels, i.e., retaining the same channels as either input features. After that, a gating mechanism is designed to transform it to weight matrices  $\hat{\mathbf{S}}$ , which are applied to both visual and semantic features element-wisely, forming a dynamic fusion of features across visual and

semantic domains. Formally,

$$\hat{\mathbf{S}} = \sigma([\mathbf{F}_{\text{pos\_sem}}^t, \mathbf{F}_{\text{pos\_vis}}^t] \mathbf{W}_{\text{conv}}) \quad (5)$$

$$\mathbf{F}_{\text{out}}^t = \hat{\mathbf{S}} \otimes \mathbf{F}_{\text{pos\_sem}}^t + (1 - \hat{\mathbf{S}}) \otimes \mathbf{F}_{\text{pos\_vis}}^t \quad (6)$$

where  $\sigma$  is the sigmoid function,  $\mathbf{W}_{\text{conv}} \in \mathbb{R}^{2C \times C}$  denotes the corresponding convolution.  $\otimes$  is the element-wise dot product. Note that the fusion is efficient and similar operations are also considered in (Fang et al., 2021; Yu et al., 2020).

One peculiarity of DSF is that  $\mathbf{W}_{\text{conv}}$ , the convolutional parameters, are shared across time steps and among MDCDP modules. As a consequence, DSF not only decouples the feature fusion with the previous cross-attention modeling, but also eases the network learning. We will verify its effectiveness in ablation study.

### 3.3 CDistNet

We then explain the construction of an effective text recognizer based on the proposed MDCDP. Through DSF, we get a *content-aware* representation that integrates recognition-related visual, semantic and positional clues. To enable thorough feature interaction, a stacked structure with several MDCDPs appended one-by-one is developed, where the number of stacked MD-CDPs is empirically set to 3 (will be discussed in experiments). The structure constructs a gradually precise feature-character alignment modeling by allowing the relevant features interactions thoroughly among the three feature spaces. Formally, it regards  $\mathbf{F}_{\text{out}}^{t,1}$ , the output of the first MDCDP at time step  $t$ , as the positional embedding of the next MDCDP, then sequentially generating  $\mathbf{F}_{\text{out}}^{t,2}$  and  $\mathbf{F}_{\text{out}}^{t,3}$ . At last, a linear classifier with softmax activation is applied to  $\mathbf{F}_{\text{out}}^{t,3}$  to get the prediction, i.e., the  $t$ -th decoded character.

## 4 Dataset

Following most scene text recognition methods, the text recognizer is trained on synthetic datasets and tested on widely used real datasets. To better evaluate CDistNet in recognizing difficult text, we further create two series of augmented datasets and also use them as the testbed. The datasets are elaborated as follows.

### 4.1 Augmented Datasets

We first construct two series of augmented datasets with different levels of recognition difficulties from the ICDAR2013 benchmark (IC13). Specifically, we employ horizontal and curved stretching of intensity from 1

(the smallest deformation) to 6 (the largest deformation) with an interval step of 1 to IC13 images. As a result, we obtain 12 counterparts of IC13 with different deformation intensities. We group the datasets according to the stretching type and termed them as HA-IC13 (horizontal) and CA-IC3 (curved) series, respectively. Each dataset simulates a certain degree of recognition challenge.

We elaborate the stretching details as follows. Given a text image  $I \in \mathbb{R}^{W \times H}$  as depicted in Fig.4(a), we first assign  $2(N+1)$  fiducial points equally distributed along upper and lower boundaries of the image, i.e., the green points in Fig.4(b) and (c). An  $\frac{W}{4N} \times H$  background region is also concatenated from the left side, as the first character may exceed the left boundary after the augmentation. Then, for each fiducial point  $p_i = [l_i, h_i]$  with  $h_i \in \{0, H\}$ , we generate its horizontal and curved counterparts, i.e., the moved fiducial points defined as  $p_i^{HA}$  and  $p_i^{CA}$ . They are calculated by using Equ.7 and Equ.8, respectively.

$$p_i^{HA} = [l_i + \theta_M, h_i] \quad (7)$$

$$p_i^{CA} = [l_i + \theta_M, h_i - \theta_M] \quad (8)$$

where  $\theta_M = \mu - \lambda * s$ .  $s \in \{1, 2, 3, 4, 5, 6\}$  is the deformation intensity.  $\mu \in [0, \frac{W}{4N}]$  is a random value.  $\lambda$  is set to  $\max(\frac{W}{8N}, \mu)$ , requiring  $\lambda \geq \mu$  such that  $\theta_M \leq 0$ . That is to say, all fiducial points are move to the left side in the X-axis (the horizontal case), and simultaneously the upper side in the Y-axis (the curved case), as the purple points shown in Fig.4(b) and (c). In the following, all image pixels are transformed according to the moved fiducial points using Thin-plate-splines. By using the equations, we create elastic transformations to the text image while roughly maintain the geometric layout of each character.

In Fig.5 we list two examples undergoing different horizontal and curved stretching intensities. As can be seen, recognition difficulties such as text deformation, unequally distributed characters of different levels are successfully created, while the text still remains recognizable by humans. Note that the augmentation is an extension of the work of Luo et al. (Luo et al., 2020). Compared to (Luo et al., 2020), the difference lies in that they focused on online augmentation and ignores constructing new datasets. While we generate two series of augmented datasets paying attention to horizontal and curved deformations with different intensities. The datasets have been made publicly available along with the code.

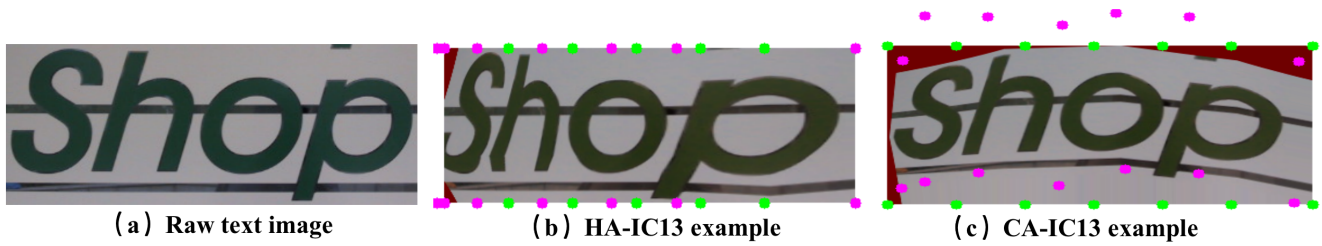


Fig. 4: Raw text image and the illustration of its augmentation. Green and purple points represent the fiducial points and their moved counterparts. (b) and (c) are the horizontal and curved stretching instances, respectively. Their deformation intensity both set to 6, the most severe one.



Fig. 5: Augmented text images in HA-IC13 (top) and CA-IC13 (bottom), which simulate horizontal and curved stretching of varying intensities, respectively.

#### 4.2 Public Datasets

Then we introduce the two synthetic datasets, and six standard benchmarks as follows.

**MJSynth (MJ)** (Jaderberg et al., 2014) and **SynthText (ST)** (Gupta et al., 2016) are two synthetic datasets each with millions of text images. 8.91M text instances from MJ and 6.95M from ST are retained for model training.

**ICDAR2013 (IC13)** is cropped from 288 scene real images. Following previous work (Baek et al., 2019), The version with 857 images is chosen for testing, which deletes non-alphanumeric characters and text shorter than 3 characters.

**Street View Text (SVT)** (Wang et al., 2011) contains 257 images for training and 647 images for testing, which are captured by Google Street View. Just testing images are chosen for our experiments.

**IIIT5k-Words (IIIT5k)** (Mishra et al., 2012) consists of 3000 testing images, which are collected from Google Image Searches. These instances are almost horizontal.

**ICDAR2015 (IC15)** (Karatzas et al., 2015) is an irregular dataset with 1811 images for testing. Words in this dataset are mostly curved, perspective and shading, which are hard to recognize.

**SVT-Perspective (SVTP)** (Phan et al., 2013) is also created from Google Street View. It contains 645 curved text images.

**CUTE80 (CT80)** (Risnumawan et al., 2014) contains 288 irregular text images cropped from natural scene images.



## 5 Experiments

### 5.1 Implementation details

We resize the text image to  $32 \times 128$  and employ the data augmentation in (Fang et al., 2021), i.e., image quality deterioration, color jitter and geometry transformation. MJ and ST datasets are used for model training. While the two series of augmented datasets and the six public datasets are retained for model assessment at different scenarios. To train CDistNet, the initial learning rate is set to  $4 \times 10^{-4}$ . The first 10k iterations use Warm-up. The whole training iterations are determined by

$$lr = d_{model}^{-0.5} \cdot \min(n^{-0.5}, n \cdot warm\_n^{-1.5}) \quad (9)$$

where  $n$  and  $warm\_n$  denote the number of normal and Warm-up iterations.  $d_{model}$  is set to 512. For ablation study and model verification, all models are trained for 6 epochs. When compared with existing methods, our model is trained for 8 epochs following Equ.9 and then another 2 epochs with a constant learning rate of  $10^{-5}$ . The batch size is set to 700.

To reduce the computational cost, we shrink the transformer units employed, where dimension of the MLP layer is reduced from 2048 to 1024 in encoder, and from 2048 to 512 in decoder. The number of encoder and decoder layers are both set to 3. Beam search is applied to determine the decoded character sequence and its size is empirically set to 10. All models are trained by using a server with 6 NVIDIA 3080 GPUs on PyTorch.

### 5.2 Ablation study

To better understand CDistNet, we carry out controlled experiments on both SVT (regular text) and IC15 (irregular text) under different configurations as follows.

**The effectiveness of SAE.** SAE imposes feature refinement on the applied branch. Besides the positional branch, it is curious that the recognition would be improved by applying SAE to the visual and semantic features on the decoder side. With this doubt in mind, we apply SAE to different branches while Tab.1 gives the result. It is seen the differences are marginal when equipping SAE to either or both visual and semantic branches (line 2,3,4). Nevertheless, on the positional branch only the improvement is noticeable (line 14). It is better than applying SAE to none or all three branches (line 1,5). The result is in line with our expectations. The visual feature is extracted from a powerful hybrid backbone while the semantic feature is dynamically fortified during decoding. It is less meaningful to

reinforce them further. In contrast, the position feature comes from a fixed embedding, while SAE allows dynamically to highlight its valuable information, especially for the subsequent MDCDP modules. Therefore improvements are observed.

**The effectiveness of CBI.** There are multiple ways to establish the CBI. We enumerate six of them and give the results in Tab.1 (line 6-10,14). CDistNet (line 14) achieves the best result among the competitors, better than the schemes that use semantic feature as the query vector, e.g., Transformer-like implementation (Sheng et al., 2019) (line 7), RobustScanner-like implementation (Yue et al., 2020) (line 9) and the scheme of using semantic feature to query position feature (S\_P, line 10). The results basically validate two hypotheses. First, imposing the positional clue on the visual branch is helpful. Second, it is effective to query semantic feature by using position feature, which perceives the semantic affinities between previous decoded characters and the character to be recognized.

**The effectiveness of DSF.** We have tested four operations to fuse the position-enhanced visual and semantic features. As shown in Tab.1, DSF outperforms static-based fusions (Add and Dot) (line 11,12) as well as the scheme that not sharing weights among MDCDP modules (line 13), demonstrating the effectiveness of the proposed scheme.

**The number of MDCDP modules considered.** Generally, stacking more MDCDPs trends to generate comprehensive feature representation, but increases the computational cost. Ablation study on this point is given by Tab.2 (the top half), where recognition accuracy and inference speed are both presented. The best accuracy is reported when three MDCDPs are equipped. It performs better than other cases where fewer (one and two) or more (four) modules are considered. Therefore the MDCDP modules in CDistNet are set to 3.

### 5.3 Model Verification

**Contribution of the positional utilization.** There are several works encoding the position information. However, CDistNet differs with them not only in the position utilization but also other aspects. To make a fair comparison, we modified these methods where other differences are mostly eliminated. The results are listed in Tab.2 (the bottom half).

We explain how the methods are modified. *CDistNet w/o Sem* denotes the semantic branch is removed from CDistNet thus the position feature only queries the visual feature (line 6 in Tab.1). The absence of modeling semantic clue, despite faster, leads to a noticeable accu-

Table 1: Ablation studies on SAE, CBI and DSF. Sem, Vis and Pos denote the semantic, visual and positional branches, respectively. S\_V denotes using semantic feature to *query* visual feature. The others are similarly defined. (✓) means switching the roles of the two features. WS denotes weight sharing among MDCDP modules.

Ablation Part	Line	SAE			CBI			Fusion	SVT	IC15
		Sem	Vis	Pos	S_V	P_V	P_S			
SAE	1					✓	✓	DSF	92.27	84.92
	2	✓				✓	✓	DSF	92.89	84.70
	3		✓			✓	✓	DSF	93.04	84.65
	4	✓	✓			✓	✓	DSF	93.04	84.76
	5	✓	✓	✓		✓	✓	DSF	93.66	84.70
CBI	6			✓		✓		DSF	90.26	82.11
	7			✓	✓			DSF	91.34	84.04
	8			✓	✓		✓	DSF	92.27	85.37
	9			✓	✓	✓		DSF	92.89	84.93
	10			✓	✓	✓	(✓)	DSF	93.35	84.70
DSF	11			✓		✓	✓	Add	91.96	85.48
	12			✓		✓	✓	Dot	91.81	84.21
	13			✓		✓	✓	DSF w/o WS	93.51	85.04
	14			✓		✓	✓	DSF	<b>93.66</b>	<b>85.92</b>

Table 2: Quantitative comparison of different methods. \* denotes our implementation with improved accuracy. Bracket values are accuracy improvements compared with results reported by their papers.

Method	#MDCDP	SVT	IC15	Speed (ms)
CDistNet	1	92.74	84.82	61.48
CDistNet	2	<b>94.28</b>	84.87	87.68
CDistNet	3	93.66	<b>85.92</b>	123.28
CDistNet	4	93.82	84.43	149.99
CDistNet w/o Sem	3	90.26	82.11	80.91
Transformer*(Sheng et al., 2019)	–	91.34 (-0.16)	84.04 (+5.00)	122.74
RobustScanner*(Yue et al., 2020)	–	91.96 (+3.86)	84.21 (+7.11)	122.78

Table 3: Quantitative comparison of different methods on HA-IC13 (left) and CA-IC13 (right). H1 denotes HA-IC13 with stretching intensity 1. The others defined similarly.

Method	Raw	H1	H2	H3	H4	H5	H6	C1	C2	C3	C4	C5	C6
Transformer*(Sheng et al., 2019)	<b>97.2</b>	96.3	95.5	92.4	86.5	79.4	72.5	95.7	94.4	85.9	75.9	65.9	58.6
RobustScanner*(Yue et al., 2020)	96.9	96.2	95.3	93.2	88.9	81.1	71.5	95.2	94.9	85.3	76.6	68.4	60.8
VisionLAN(Wang et al., 2021)	96.3	93.6	92.9	90.0	82.3	72.2	61.0	94.9	92.8	84.0	75.0	64.3	52.7
ABINet(Fang et al., 2021)	97.0	95.9	95.2	92.0	85.8	73.8	65.0	<b>96.6</b>	<b>95.9</b>	87.9	76.3	65.5	54.5
CDistNet	97.1	<b>96.6</b>	<b>96.2</b>	<b>94.3</b>	<b>90.0</b>	<b>83.4</b>	<b>77.7</b>	96.3	95.6	<b>88.5</b>	<b>79.6</b>	<b>70.4</b>	<b>63.1</b>

racy drop of over 3% on average. It implies the importance of semantic feature. In *Transformer\** (line 7 in Tab.1), we strengthen the raw implementation (Sheng et al., 2019) using our visual encoding branch, from which 5% accuracy gain in IC15 is observed due to a superior visual feature. Besides the visual encoding branch, *RobustScanner\** uses our Transformer unit to replace its "CNN+LSTM" implementation. It improves the accuracy by 3.86% and 7.11% on SVT and IC15, respectively. Our modification leads to noticeable improvements to their raw implementations.

With the modifications, accuracy gains from the position modeling can be quantitatively evaluated. CDistNet still attains nearly 1.7% accuracy gains on average in both datasets compared with *RobustScanner\**, largely attributed to that P\_S (i.e., using position fea-

ture to query semantic feature) is a superior cross-attention scheme compared to S\_V (i.e., using semantic feature to query visual feature).

**Performance on augmented datasets.** As described, HA-IC13 and CA-IC13 are simulated with different horizontal and curved deformation intensities, forming test-bed with increasing difficulties, a nearly ideal scenario for assessing CDistNet in recognizing difficult text.

We validate CDistNet in both series of datasets and Tab.3 presents the results, where ABINet (Fang et al., 2021) and VisionLAN (Wang et al., 2021) are two leading models in standard benchmarks. All methods recognize well in raw IC13 due to its simplicity. With the rise of deformation intensity, CDistNet shows its superiority. It goes down slower. The accuracy gaps gradually become larger with the intensity increase, where mar-

Table 4: Accuracy comparison with existing methods on six standard benchmarks.

Method	Year	Training Data	IC13	SVT	IIITK	IC15	SVTP	CT80
CRNN(Shi et al., 2017)	2017	90K	86.7	80.8	78.2	–	–	–
FocusAtten(Cheng et al., 2017)	2017	90K+ST	93.3	85.9	87.4	70.6	–	–
AON(Cheng et al., 2018)	2018	90K+ST	–	82.8	87.0	68.2	73.0	76.8
ASTER(Shi et al., 2018)	2018	90K+ST	91.8	89.5	93.4	76.1	78.5	79.5
ESIR(Zhan and Lu, 2019)	2019	90K+ST	91.3	90.2	93.3	76.9	79.6	83.3
SAR(Li et al., 2019)	2019	90K+ST	91.0	84.5	91.5	69.2	76.4	83.3
2D-Attention(Lyu et al., 2019)	2019	90K+ST	92.7	90.1	94.0	76.3	82.3	86.8
MaskTextSpotter(Liao et al., 2019)	2019	90K+ST	95.3	90.6	93.9	77.3	82.2	87.8
NRTR(Sheng et al., 2019)	2019	90K+ST	95.8	91.5	90.1	79.4	86.6	80.9
SE-ASTER (Qiao et al., 2020)	2020	90K+ST	92.8	89.6	93.8	80.0	81.4	83.6
Textscanner(Wan et al., 2020)	2020	90K+ST	92.9	90.1	93.9	79.4	84.3	83.3
DAN(Wang et al., 2020)	2020	90K+ST	93.9	89.2	94.3	74.5	80.0	84.4
RobustScanner(Yue et al., 2020)	2020	90K+ST	94.8	88.1	95.3	77.1	79.5	90.3
SRN(Yu et al., 2020)	2020	90K+ST	95.5	91.5	94.8	82.7	85.1	87.8
Pren2D(Yan et al., 2021)	2021	90K+ST+Real	96.4	94	95.6	83	87.6	91.7
JVSR(Bhunja et al., 2021)	2021	90K+ST	95.5	92.2	95.2	84.0	85.7	89.7
VisionLAN(Wang et al., 2021)	2021	90K+ST	95.7	91.7	95.8	83.7	86.0	88.5
ABINet(Fang et al., 2021)	2021	90K+ST	<b>97.4</b>	93.5	96.2	<b>86.0</b>	<b>89.3</b>	89.2
S-GTR(He et al., 2022)	2022	90K+ST	96.8	<b>94.1</b>	95.8	84.6	87.9	92.3
CDistNet (Ours)	–	90K+ST	<b>97.4</b>	93.5	<b>96.4</b>	<b>86.0</b>	88.7	<b>93.4</b>

gins ranging from 5.2% to 16.7%, and from 2.3% to 10.4% are respectively observed compared with other methods in HA-IC13 with intensity 6 (H6) and CA-IC13 with intensity 6 (C6). Noticing that existing leading models perform near saturation in public benchmarks, where the accuracy gap is not obvious (elaborated later) and might not be enough to well distinguish these methods. The remarkable gap clearly verifies the great generalization ability of CDistNet especially in recognizing difficult text. The argumentation generates many unequally spaced and severely bent characters. However, CDistNet shows much better robustness to these challenges due to perceiving character distances in both visual and semantic domains.

We also observe that the sequential decoding methods behave differently from the parallel decoding ones. ABINet and VisionLAN, which employ the parallel decoding scheme for speed acceleration, experience even sharp decreases compared to the three sequential decoding methods. For example, CDistNet is better than VisionLan and ABINet by 16.7% and 12.7% in H6, 10.4% and 8.6% in C6. Transformer\* and RobustScanner\* also have large margins compared to them. The significant accuracy gaps can be explained as not only their positional embedding is content-free, but also their parallel decoding schemes are established at the cost of sacrificing the attention quality in difficult text. Note that we are the first observing the inefficiency of popular parallel decoding schemes in handling difficult text. Tackling the drawback should be an interesting topic worthy of further study.

#### 5.4 Comparisons with Existing Methods

We compare CDistNet with nineteen existing methods published from year 2017 to 2022, covering the majority of influential methods of these years. The results are given by Tab.4. It is shown that CDistNet achieves the best results on four datasets including IC13, IIITK, IC15 and CT80. As expected, the performance gains are more prominent in irregular text datasets compared to regular text datasets, demonstrating its superiority in modeling challenging characters. When comparing with previously state-of-the-art methods such as ABINet and S-GTR, CDistNet does not always show obvious accuracy differences (i.e., within 1% in five of the six datasets) although consistently ranks top-tier. It indicates that the performance of scene text recognition is approaching saturate on these benchmarks. When looking into the closely related sequential decoding methods (Sheng et al., 2019; Wan et al., 2020; Yue et al., 2020), CDistNet outperforms them by large margins on all six datasets. It again demonstrates the superiority of the proposed feature modeling. It incorporates visual, semantic and positional clues that model fine-grained character distance. It, thus, better aligns the feature-character information even with various recognition difficulties.

#### 5.5 Decoding Visualization

We visualize three illustrative examples in the form of semantic affinity matrices in Fig.6, where the semantic utilization of three different methods (i.e., Trans-

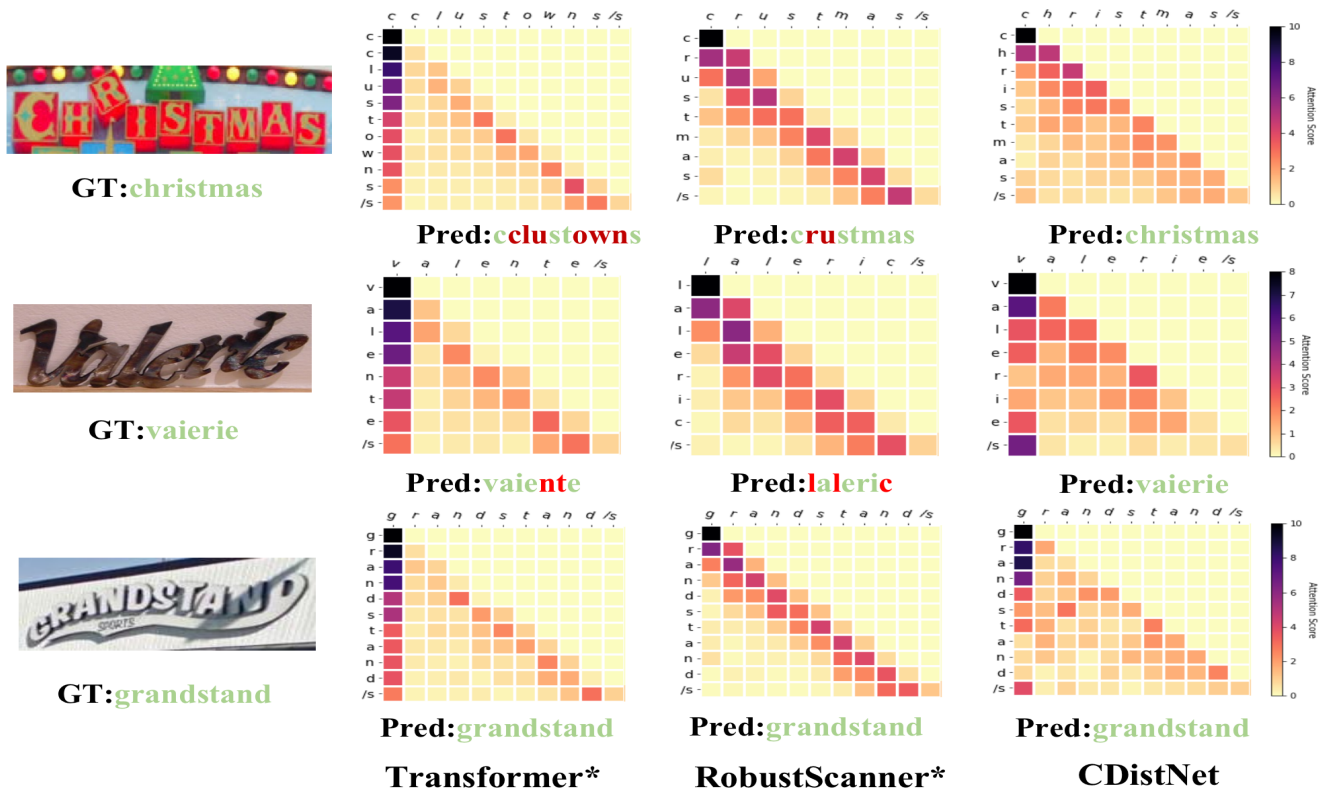


Fig. 6: Visualization of the semantic affinity matrices of different methods. In each matrix a row represents the semantic affinities between previously decoded characters and the diagonal character to be decoded. Darker color indicates higher affinity value. The leftmost column is the text image and groundtruth. The second to fourth columns correspond to visualizations of Transformer\*, RobustScanner\* and CDistNet. Red color means incorrectly recognized characters.

former\*, RobustScanner\* and CDistNet) during the decoding are shown. They are obtained by inspecting their respective (position-enhanced) semantic branches.

Specifically, in each matrix, Y-axis denotes the decoding time steps while X-axis represents the decoded characters. Darker color indicates higher affinity value, i.e., higher contribution in recognizing the diagonal character. Two observations are obtained from the matrices. First, the diagonal elements play more important roles (darker) in CDistNet than the other two methods. Since CDistNet jointly models recognition clues in visual, semantic and position spaces, the feature is more aware of the character to be recognized. It is thus more confident in semantic utilization. Second, for CDistNet the majority of previous decoded characters have darker color thus more deeply contributing to the decoding process. It produces more accurate prediction in general. On the contrary, in Transformer\* the position and semantic features are not well decoupled. So the decoding mostly relies on the first column. While in RobustScanner\*, although the position is decoupled, the decoding less considers characters far from the recognized one. It

implies in part why the two methods sometimes make incorrect recognition. Conversely, again demonstrating that CDistNet achieves a more comprehensive semantic affinity utilization.

We then visualize the attention map based on the position-enhanced visual branch of the last MDCDP, where six examples are shown in Fig.7. The characters are properly localized on the attention maps in most cases. It implies that CDistNet retains powerful and universal recognition capability with the existence of various difficulties. The joint feature representation well encodes the spatial layout and semantic affinity among characters, thus ensuring that accurate feature-character alignments are established at most time steps. On the other hand, it is observed that there are also a few wrongly recognized cases. The failures can be summarized as three categories mainly, i.e., multiple text fonts (e.g., harry), severe blur (e.g., quilts) and vertical text. Most of them are even indistinguishable by humans and they are still common challenges for modern text recognizers.

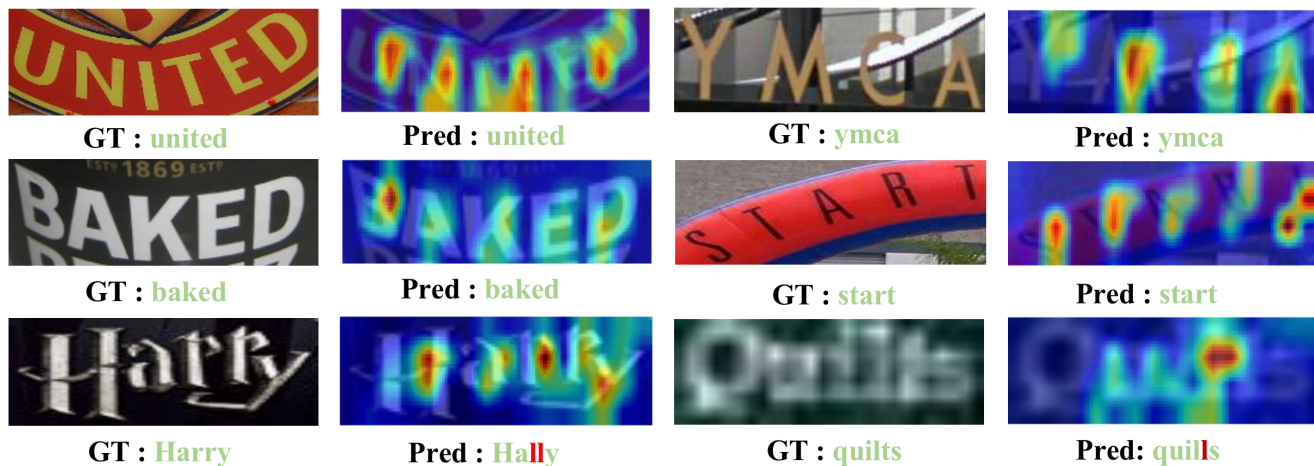


Fig. 7: Attention map visualization of the position-enhanced visual feature in the last MDCDP module. GT and Pred denote the ground-truth and predicted result, respectively. Red color means incorrectly recognized characters.

## 6 Conclusion

Targeting to improve the accuracy of scene text recognition especially in difficult text, we have presented the MDCDP module which utilizes position feature to *query* both visual and semantic features within the Transformer-based encoder-decoder framework. It learns a joint representation that delineates character distance in both visual and semantic domains. Accordingly, CDistNet has been developed for robust scene text recognition. We have carried out extensive experiments to verify its effectiveness. While ablation studies demonstrate the effect of each proposed component. The comparison results successfully validate our proposal. It not only reports state-of-the-art accuracy when compared with existing methods on six standard benchmarks, but also on two series of augmented datasets it shows greater advantages as the deformation intensity increases. In addition, the visualization experiments verify that superior attention localization and reasonable semantic utilization are reached in visual and semantic domains, respectively.

Accuracy and inference speed are always two key metrics for scene text recognition. It is observed that the accuracy on existing public benchmarks is near saturation, which might be insufficient to well distinguish the methods performed top-tier. Our study reveals these methods differ significantly on severely deformed HA-IC13 and CA-IC13 datasets. We hope the datasets can foster future research in designing robust scene text recognition models. Meanwhile, some recent studies reported very fast yet efficient solutions by leveraging the vision transformer architecture (Du et al., 2022; Li et al., 2022). Thus, we are also interested in developing

methods to accelerate the recognition by following this pipeline.

**Acknowledgements** This work was supported by the National Natural Science Foundation of China under Grants 62172103 and 62102384.

## References

- Baek J, Kim G, Lee J, Park S, Han D, Yun S, Oh SJ, Lee H (2019) What is wrong with scene text recognition model comparisons? dataset and model analysis. In: ICCV, pp 4714–4722
- Bai J, Chen Z, Feng B, Xu B (2014) Chinese image text recognition on grayscale pixels. In: 2014 IEEE International Conference on Acoustics, Speech and Signal Processing (ICASSP), IEEE, pp 1380–1384
- Bhunia AK, Sain A, Kumar A, Ghose S, Chowdhury PN, Song YZ (2021) Joint visual semantic reasoning: Multi-stage decoder for text recognition. In: ICCV, pp 14920–14929
- Chen X, Wang T, Zhu Y, Jin L, Luo C (2020) Adaptive embedding gate for attention-based scene text recognition. *Neurocomputing* 381:261–271
- Chen X, Jin L, Zhu Y, Luo C, Wang T (2021) Text recognition in the wild: A survey. *ACM Comput Surv* 54(2)
- Cheng Z, Bai F, Xu Y, Zheng G, Pu S, Zhou S (2017) Focusing attention: Towards accurate text recognition in natural images. In: ICCV, pp 5076–5084
- Cheng Z, Xu Y, Bai F, Niu Y, Pu S, Zhou S (2018) Aon: Towards arbitrarily-oriented text recognition. In: CVPR, pp 5571–5579

- Devlin J, Chang MW, Lee K, Toutanova K (2019) Bert: Pre-training of deep bidirectional transformers for language understanding. In: NAACL-HLT
- Du Y, Chen Z, Jia C, Yin X, Zheng T, Li C, Du Y, Jiang Y (2022) SVTR: scene text recognition with a single visual model. arXiv preprint arXiv:220500159
- Fang S, Xie H, Wang Y, Mao Z, Zhang Y (2021) Read like humans: Autonomous, bidirectional and iterative language modeling for scene text recognition. In: CVPR, pp 7094–7103
- Gupta A, Vedaldi A, Zisserman A (2016) Synthetic data for text localisation in natural images. In: CVPR, pp 2315–2324
- He P, Huang W, Qiao Y, Loy CC, Tang X (2016) Reading scene text in deep convolutional sequences. In: AAAI
- He Y, Chen C, Zhang J, Liu J, He F, Wang C, Du B (2022) Visual semantics allow for textual reasoning better in scene text recognition. In: AAAI
- Hu W, Cai X, Hou J, Yi S, Lin Z (2020) Gtc: Guided training of ctc towards efficient and accurate scene text recognition. In: AAAI, vol 34, pp 11005–11012
- Jaderberg M, Simonyan K, Vedaldi A, Zisserman A (2014) Synthetic data and artificial neural networks for natural scene text recognition. arXiv preprint arXiv:14062227
- Jaderberg M, Simonyan K, Vedaldi A, Zisserman A (2016) Reading text in the wild with convolutional neural networks. *International Journal of Computer Vision* 116(1):1–20
- Karatzas D, Shafait F, Uchida S, Iwamura M, Bigorda LG, Mestre SR, Mas J, Mota DF, Almazan JA, De Las Heras LP (2013) Icdar 2013 robust reading competition. In: ICDAR, pp 1484–1493
- Karatzas D, Gomez-Bigorda L, Nicolaou A, Ghosh S, Bagdanov A, Iwamura M, Matas J, Neumann L, Chandrasekhar VR, Lu S, et al. (2015) Icdar 2015 competition on robust reading. In: ICDAR, pp 1156–1160
- Lan Z, Chen M, Goodman S, Gimpel K, Sharma P, Soricut R (2019) Albert: A lite bert for self-supervised learning of language representations. arXiv preprint arXiv:190911942
- Lee CY, Osindero S (2016) Recursive recurrent nets with attention modeling for ocr in the wild. In: CVPR, pp 2231–2239
- Li C, Liu W, Guo R, Yin X, Jiang K, Du Y, Du Y, Zhu L, Lai B, Hu X, Yu D, Ma Y (2022) Pp-ocrv3: More attempts for the improvement of ultra lightweight OCR system. arXiv preprint arXiv:220603001
- Li H, Wang P, Shen C, Zhang G (2019) Show, attend and read: A simple and strong baseline for irregular text recognition. In: AAAI, vol 33, pp 8610–8617
- Li Y, Qi H, Dai J, Ji X, Wei Y (2017) Fully convolutional instance-aware semantic segmentation. In: CVPR, pp 2359–2367
- Liao M, Lyu P, He M, Yao C, Wu W, Bai X (2019) Mask textspotter: An end-to-end trainable neural network for spotting text with arbitrary shapes. *IEEE Transactions on Pattern Analysis and Machine Intelligence* 43(2):532–548
- Liao M, Zhang J, Wan Z, Xie F, Liang J, Lyu P, Yao C, Bai X (2019) Scene text recognition from two-dimensional perspective. In: AAAI, vol 33, pp 8714–8721
- Long S, He X, Yao C (2021) Scene text detection and recognition: The deep learning era. *International Journal of Computer Vision* 129(1):161–184
- Luo C, Jin L, Sun Z (2019) MORAN: A multi-object rectified attention network for scene text recognition. *Pattern Recognition* 90:109–118
- Luo C, Zhu Y, Jin L, Wang Y (2020) Learn to augment: Joint data augmentation and network optimization for text recognition. In: CVPR, pp 13746–13755
- Luo C, Lin Q, Liu Y, Jin L, Shen C (2021) Separating content from style using adversarial learning for recognizing text in the wild. *International Journal of Computer Vision* 129(4):960–976
- Lyu P, Liao M, Yao C, Wu W, Bai X (2018) Mask textspotter: An end-to-end trainable neural network for spotting text with arbitrary shapes. In: ECCV, pp 67–83
- Lyu P, Yang Z, Leng X, Wu X, Li R, Shen X (2019) 2d attentional irregular scene text recognizer. arXiv preprint arXiv:190605708
- Mishra A, Alahari K, Jawahar C (2012) Scene text recognition using higher order language priors. In: BMVC, pp 1–11
- Nguyen N, Nguyen T, Tran V, Tran MT, Ngo TD, Nguyen TH, Hoai M (2021) Dictionary-guided scene text recognition. In: CVPR, pp 7383–7392
- Phan TQ, Shivakumara P, Tian S, Tan CL (2013) Recognizing text with perspective distortion in natural scenes. In: ICCV, pp 569–576
- Qiao Z, Zhou Y, Yang D, Zhou Y, Wang W (2020) Seed: Semantics enhanced encoder-decoder framework for scene text recognition. In: CVPR, pp 13525–13534
- Risnumawan A, Shivakumara P, Chan CS, Tan CL (2014) A robust arbitrary text detection system for natural scene images. *ESA* 41(18):8027–8048
- Rodriguez-Serrano JA, Gordo A, Perronnin F (2015) Label embedding: A frugal baseline for text recognition. *International Journal of Computer Vision* 113(3):193–207
- Sheng F, Chen Z, Xu B (2019) Nrtr: A no-recurrence sequence-to-sequence model for scene text recogni-

- tion. In: ICDAR, pp 781–786
- Shi B, Bai X, Yao C (2017) An end-to-end trainable neural network for image-based sequence recognition and its application to scene text recognition. *IEEE Transactions on Pattern Analysis and Machine Intelligence* 39(11):2298–2304
- Shi B, Yang M, Wang X, Lyu P, Yao C, Bai X (2018) Aster: An attentional scene text recognizer with flexible rectification. *IEEE Transactions on Pattern Analysis and Machine Intelligence* 41(9):2035–2048
- Su B, Lu S (2017) Accurate recognition of words in scenes without character segmentation using recurrent neural network. *Pattern Recognition* 63:397–405
- Vaswani A, Shazeer N, Parmar N, Uszkoreit J, Jones L, Gomez AN, Kaiser L, Polosukhin I (2017) Attention is all you need. In: NIPS, pp 5998–6008
- Wan Z, He M, Chen H, Bai X, Yao C (2020) Textscanner: Reading characters in order for robust scene text recognition. In: AAAI, vol 34, pp 12120–12127
- Wang K, Babenko B, Belongie S (2011) End-to-end scene text recognition. In: ICCV, pp 1457–1464
- Wang P, Yang L, Li H, Deng Y, Shen C, Zhang Y (2019a) A simple and robust convolutional-attention network for irregular text recognition. arXiv preprint arXiv:190401375 6:2
- Wang S, Wang Y, Qin X, Zhao Q, Tang Z (2019b) Scene text recognition via gated cascade attention. In: ICME, pp 1018–1023
- Wang T, Zhu Y, Jin L, Luo C, Chen X, Wu Y, Wang Q, Cai M (2020) Decoupled attention network for text recognition. In: AAAI, vol 34, pp 12216–12224
- Wang Y, Xie H, Fang S, Wang J, Zhu S, Zhang Y (2021) From two to one: A new scene text recognizer with visual language modeling network. In: ICCV, pp 14174–14183
- Xing L, Tian Z, Huang W, Scott MR (2019) Convolutional character networks. In: ICCV, pp 9126–9136
- Yan R, Peng L, Xiao S, Yao G (2021) Primitive representation learning for scene text recognition. In: CVPR, pp 284–293
- Ye Q, Doermann D (2014) Text detection and recognition in imagery: A survey. *IEEE Transactions on Pattern Analysis and Machine Intelligence* 37(7):1480–1500
- Yu D, Li X, Zhang C, Liu T, Han J, Liu J, Ding E (2020) Towards accurate scene text recognition with semantic reasoning networks. In: CVPR, pp 12113–12122
- Yue X, Kuang Z, Lin C, Sun H, Zhang W (2020) Robustscanner: Dynamically enhancing positional clues for robust text recognition. In: ECCV, pp 135–151
- Zhan F, Lu S (2019) Esir: End-to-end scene text recognition via iterative image rectification. In: CVPR, pp

2059–2068